Crystallization of Syndiotactic Polystyrene in β-Form. 1. Positional Identification of Stacking Faults in the Solution-Grown Single Crystals

Masatoshi Tosaka,* Noritaka Hamada,† Masaki Tsuji, Shinzo Kohjiya, Tetsuya Ogawa, Seiji Isoda, and Takashi Kobayashi

Division of States and Structures, Institute for Chemical Research, Kyoto University Uji, Kyoto-fu 611, Japan

Received January 13, 1997[⊗]

ABSTRACT: The locations of the stacking faults in β-form single crystals of syndiotactic polystyrene, which were grown isothermally from a dilute solution at temperatures ranging from 150 to 210 °C, were identified in high-resolution and dark-field (DF) images taken by transmission electron microscopy. The shift or kink of the (210) lattice fringes, which shows the position of the fault, was directly detected in the high-resolution images. DF images taken using several reflections exhibited irregularly spaced striations parallel to the *b*-axis. Computer simulation of DF images based on the structural model of the stacking fault well supported the view that each striation corresponds to the position of the fault. The striations extended continuously and were very long, and accordingly, it was proposed that the stacking fault influences the attachment of a new polymer stem onto the lateral growth face which is not parallel to the *bc*-plane, resulting in irregular fold-surfaces of the single crystals.

Introduction

Syndiotactic polystyrene (s-PS) is known to present a complicated polymorphic behavior. The phase-transition behavior and its characterization were studied in various publications.[1−9] Most of them reported that when s-PS is crystallized in the presence of solvent, the polymer chains adopt a (2/1)2 helical conformation (TTGG) and s-PS forms a molecular compound incorporating the solvent molecules. If the molecular compound is dried and annealed, *e.g.* at a temperature higher than 180 °C, then the solvent molecules are removed from the compound and the conformation of polymer chains is accordingly changed into the planar-zigzag one (TTTT). Guerra *et al.* classified the polymorphism of s-PS into four modifications[3], in which the β-form is distinguished by the orthorhombic unit cell and the planar-zigzag conformation of the polymer chain. The crystal structure of β-form was already analyzed by Chatani *et al.*[10] and De Rosa *et al.*[11] Chatani *et al.* prepared the sample for X-ray analysis by annealing the uniaxially oriented s-PS/toluene molecular-compound above 200 °C. While most of the researchers prepared β-form samples in a similar manner, as above, we have grown β-form single crystals of s-PS isothermally from a dilute solution.[12] It should be noted, therefore, that the β-form sample can be directly obtained even in the presence of solvent. The selected-area electron diffraction (ED) pattern from the single crystal indicated, referring to the crystal structure proposed by Chatani *et al.*, that the molecular chains are set perpendicular to the basal surface of the single-crystal platelet, namely its lamellar surface. The ED pattern also indicated that the β-form single crystal involves stacking faults in its molecular-stem packing: the presence of the faults is deduced from the streaked feature of certain reflections observed in the ED pattern, as shown in Figure 1. This feature was inevitably found in every β-form single crystal in our experiment. The *ab*-projection of the proposed crystal structure with the

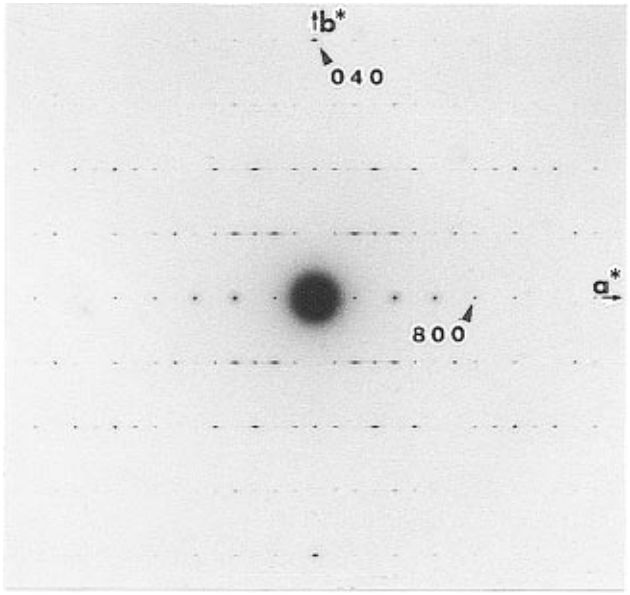

Figure 1. ED pattern from the s-PS β-form single crystal grown at 200 °C.

fault is shown in Figure 2, in which a rectangle designated with broken lines means the unit cell. Here it is noted that our assignment of *a* and *b* directions is different from that proposed by Chatani *et al.*[10] and De Rosa *et al.*[11]

In the ED patterns of the β-form single crystal (for example, Figure 1), *hk*0 reflections with $h + k =$ even are spotlike, while the others with $h + k =$ odd are streaked along the *a**-direction. We have proposed a model of the defect structure[12] to explain the characteristic features of the ED pattern. In the model, the regular structure of the β-form is composed of two types of motifs: Each motif is composed of two monomolecular layers extended parallel to the *bc*-plane (of course, the thickness of every motif in the *c*-direction approximately equals the lamellar thickness of single crystals grown isothermally at a given crystallization temperature). The motifs are distinguished each other by the rotational orientation of the backbone chain. These two

* To whom all correspondence should be addressed.
† Yamanouchi Pharmaceutical Co., Ltd.
⊗ Abstract published in *Advance ACS Abstracts,* June 15, 1997.

S0024-9297(97)00024-7 CCC: $14.00

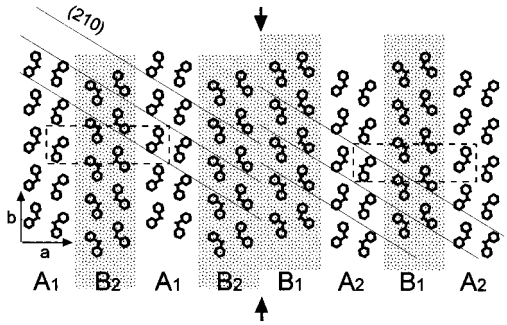

Figure 2. Schematic drawing of the *ab*-projection of the s-PS β-form crystal structure with the stacking fault. The unit cell of the regular structure is shown by a rectangle drawn with broken lines. Motifs B are shaded. A pair of arrows indicate the position of the stacking fault. Oblique straight lines indicate the (210) lattice planes in both sides of the fault. The shift of (210) planes by half of the spacing is well demonstrated.

types of motifs were named A and B for convenience as shown in Figure 2, in which subscripts (1 and 2) show whether or not the motif is relatively shifted along the *b*-axis by half a period. Thus the regular structure is defined as an alternating stack of these two motifs, that is, both sequences, $-A_1B_2A_1B_2-$ and $-A_2B_1A_2B_1-$, correspond to the regular crystal lattice. When a sequence having two motifs of the same type in succession is incorporated in a stack, such as $-B_1A_2A_1B_2-$ or $-A_1B_2B_1A_2-$, then this sequence is regarded as the stacking fault. The number of stacking faults, for example, in the sequence $-B_1A_2A_1A_2A_1B_2-$ or $-A_1B_2B_1B_2B_1A_2-$ is "three". Theoretical formulation of the intensity distribution based on this model explained sufficiently the characteristic features observed in the ED pattern.[12]

In the structural study described above, which was mainly based on the analysis of the ED pattern, the lateral size of the crystal platelet was assumed to be very large. Accordingly, the plane of the stacking fault was assumed to go through the platelet from one edge to the other in a direction parallel to the *b*-axis. However, if multiple nucleation occurs on one (100) plane in both regular and faulted ways, spreading of the plane of the faulted structure in the *b*-axis direction will be interrupted by the regular one, and thus the length of the plane in question will become small. In order to know whether this situation really occurs or not, the length of the plane of the faulted structure along the *b*-direction must be examined. In the *ab*-projection of the crystal platelet, this length, of course, corresponds to the length of a "line" indicating the location of the stacking fault. For this purpose, therefore, it is necessary to identify the location of the fault. Hence we again adopt transmission electron microscopy (TEM). The structural information on the stacking fault is to be included in the streaked reflections in the ED pattern. Dark-field (DF) images produced by using these streaked reflections are, therefore, to give useful information to study the arrangement of the planes of faulted structure. On the other hand, as demonstrated in the previous work,[12] it is possible to obtain high-resolution electron microscopic (HREM) images of this crystal and to detect directly the location of the stacking faults from the images.

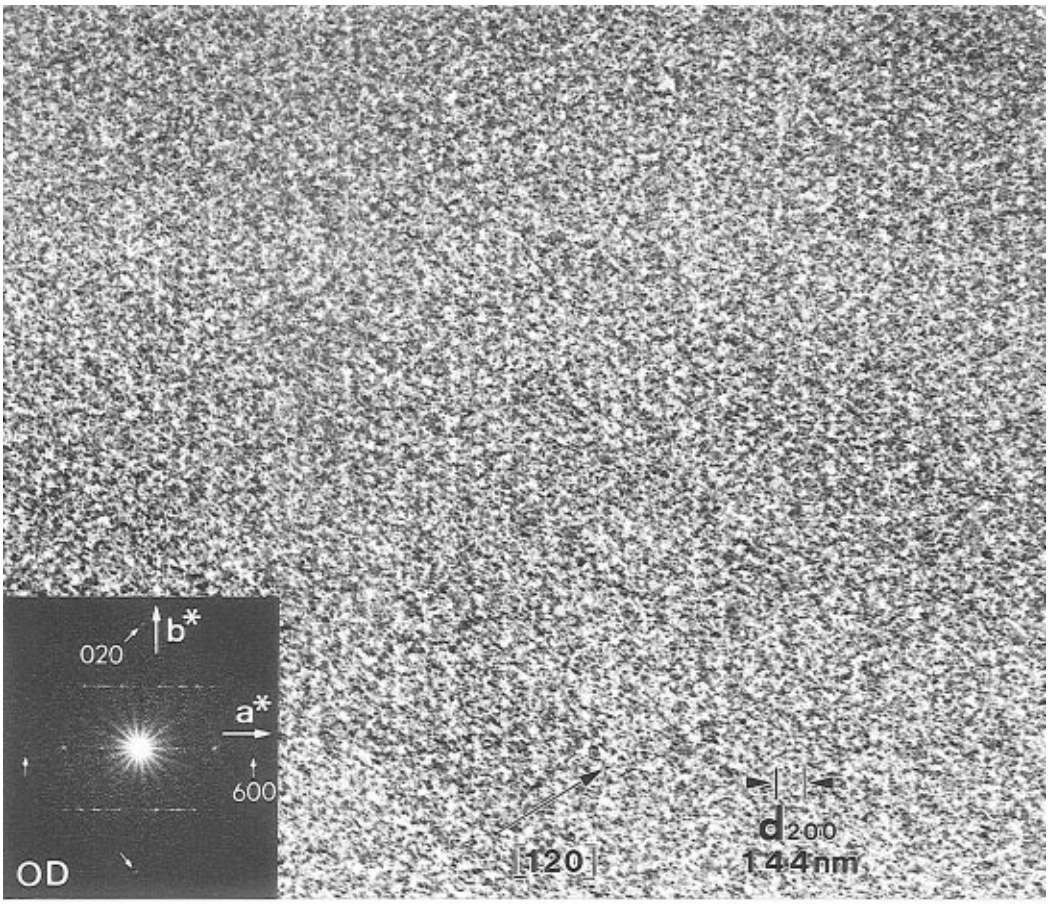

Figure 3. HREM image of the s-PS β-form single crystal grown at 205 °C, which was taken at 4.2 K with a cryogenic transmission electron microscope. The inset is the optical diffractogram of the original negative, showing the same streaked feature as in the ED pattern (Figure 1) from the crystal.

In the present work, these TEM techniques are utilized to investigate the arrangement of the stacking faults. Since we really found irregularly spaced straight striations in the DF images, a computer simulation for the DF imaging is performed in order to identify the origin of such striations. On the basis of these results, the structure of the β-form single crystal of s-PS is discussed. More detailed morphological features, which were not described in the previous publication,[12] will also be reported.

Experimental Section

The s-PS ($M_w = 7 \times 10^4$) sample was kindly supplied by Idemitsu Petrochemical Co., Ltd. and was used without further purification. A mixture of *n*-tetradecane and decahydronaphthalene (2:1 v/v) was used as the solvent. The specimen was prepared by the following procedure. First, an 0.01 wt % solution of s-PS was prepared by dissolving the sample in the boiling solvent. Meantime, an NaCl crystal was newly cleaved and preheated in the sample-free solvent. Then the NaCl crystal as a substrate was quickly transferred into the solution, which was thermostated at a desired crystallization temperature ranging from 150 to 225 °C. After isothermal crystallization for 2 h, the NaCl crystal was taken out of the solution, rinsed with the hot solvent maintained at the same temperature, and dried in an ambient atmosphere. Single crystals of s-PS thus grown on the newly cleaved (001) face of NaCl were comparatively flat and suitable for TEM. No epitaxial feature has been found between the NaCl and the s-PS crystals.[12] The s-PS crystals on NaCl were reinforced with a vacuum-evaporated carbon film. The NaCl with s-PS crystals was put into water, and the s-PS specimen was floated away from the NaCl and picked up onto a copper grid for TEM.

DF images were taken with a conventional transmission electron microscope (JEOL JEM-200CS operated at 200 kV) by using several reflections (both spotlike and streaked) at a direct magnification of 5×10^3. Kodak SO-163 films were used for recording the DF images and developed at 20 °C for 5 min in full-strength Mitsubishi Gekkol developer. HREM images were taken with a cryogenic transmission electron microscope (JEOL JEM-4000SFX operated at 400 kV) equipped with a built-in minimum-dose system (MDS) at a direct magnification of 1×10^5. In this case, specimens mounted on the gold-coated microgrids[12] were cooled down to liquid-helium temperature (4.2 K) to suppress radiation damage, and the electron dose on the specimen for taking one micrograph was set at 7×10^3 electrons/nm^2 for the SO-163 films, which were developed at 20 °C for 10 min in the same developer.

Computer simulations of DF images were performed on personal computers. The potential distribution that represents the *ab*-projection of the crystal lattice with stacking faults of 25% was calculated with our original software. The potential distribution for each atom was assumed to be Gaussian. The atomic positions in the regular and faulted crystal lattices were quoted from ref 10. The simulation was performed with a Fourier filtering technique provided in a commercial software package (DigitalMicrograph version 2.5.6, Gatan Inc.).

Results and Discussion

Single crystals of s-PS were successfully obtained at crystallization temperatures below 210 °C. Most of the crystals were multilayered, but a few monolayered crystals were also obtained. Well-defined single crystals were always truncated-lozenge shaped. They had, however, curved growth faces with no sharp corners. Hence their growth faces were not identified in the crystallographic sense, except for the (100) plane as truncation faces. These features are essentially the same as the crystals presented in ref 12. Cracks and pleats were newly observed, however, in this experiment, in some of the monolayered crystals and in monolayered regions of the basal platelet of a multilayered crystal. They may be caused by collapse of the nonplanar lamellar crystal.

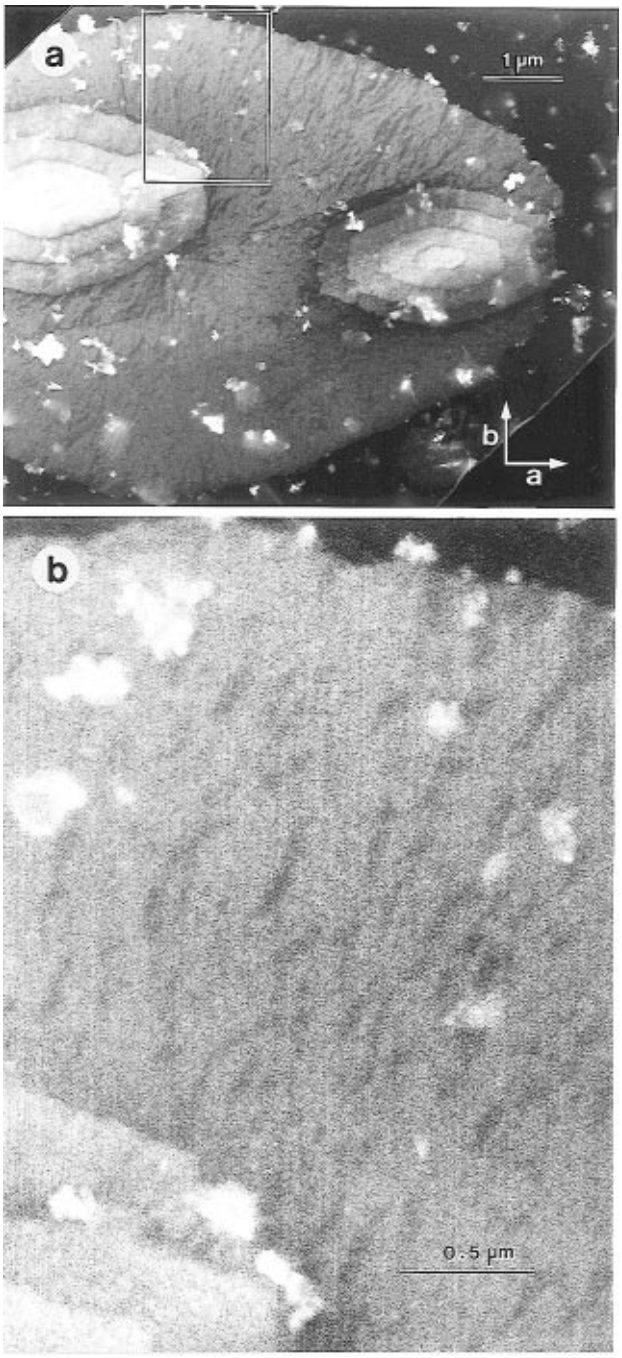

Figure 4. (a) DF image of the s-PS single crystal grown at 165 °C. (b) Enlarged photograph from the rectangular area in part a. Irregularly spaced straight striations parallel to the *b*-axis direction can be seen.

HREM Images. Figure 3 is an example of the HREM images of the single crystal grown isothermally at 205 °C, which give the same streaked feature in their optical diffraction patterns as seen in the ED pattern (Figure 1) of the single crystal. These images, hence, possess structural information on the stacking fault. However, it is very difficult to recognize the location of the stacking faults in most of the HREM images. One of the reasons is that the fault is detected only as a slight kink or shift of, for example, (210) lattice fringes as illustrated in Figure 2,[12] and the fringes are obscurely buried in the granularity of the photographic film. (In general, HREM images of organic crystals are taken at a fairly low electron dose of exposure to suppress their

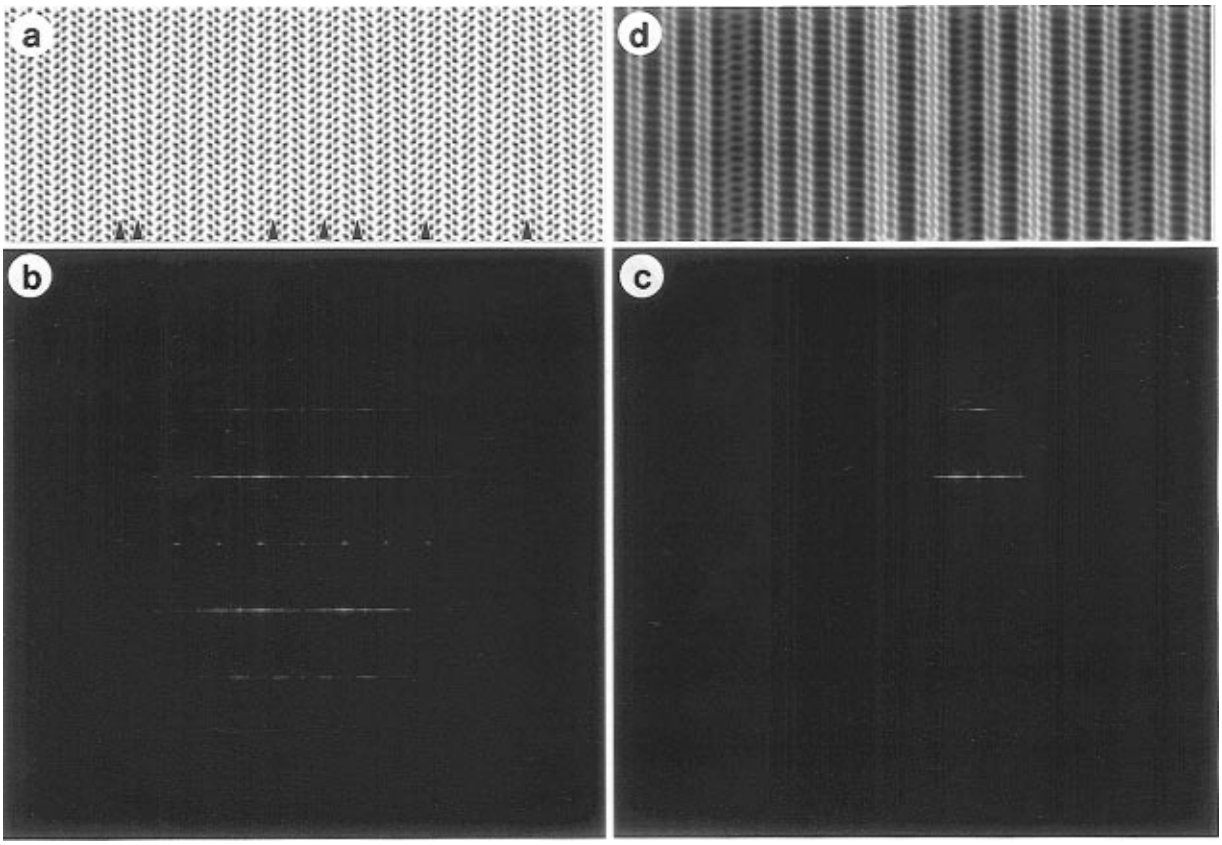

Figure 5. Simulation of the DF imaging: (a) electrostatic potential distribution of the crystal lattice with stacking faults of 25%, which is projected onto the *ab*-plane (stacking faults located at the positions indicated with arrowheads); (b) Fourier transform of part a; (c) selection of some reflections from the Fourier transform in part b with a circular aperture in the filter; (d) simulated DF image of the crystal lattice in part a, using the selected reflections in part c. Dark or bright contrast appears at the positions of the stacking faults.

radiation damage. This, accordingly, results in obscure, less clear images due to a low signal-to-noise ratio.) Another reason is that the lattice fringes in the HREM images were not uniformly recorded. That is to say, the phase and the intensity of the fringes changed continuously from place to place. This may come from slight tilt of the crystal lattice, due to the mosaic or wavy nature of the lamellae. We adopted, therefore, the following method to identify the location of the faults. A transparent sheet with regularly spaced parallel stripes was prepared. The spacing of the stripes was slightly different from that of (210) lattice fringes in the photograph enlarged from the original negative. When we put the sheet onto the HREM photograph in such a way so that the stripes become parallel to the (210) fringes, moiré fringes were generated by interference between the (210) lattice fringes and the regular stripes in the transparent sheet. Though the moiré fringes were still obscured, we could observe moving moiré fringes when we moved the sheet slowly. The position of the stacking fault could be detected as a kinked part of the moiré fringes because the part remained steady. In this way, we can estimate the probability of the presence of the stacking fault by counting the number of faults in a certain unit length in the *a*-axis direction which were recorded in the HREM images. The number is counted in the distinct coherent regions where the lattice fringes are definitely observed. The probability was about 15% for the specimen crystallized at 205 °C, that is, one stacking fault per 6.7 motifs.

DF Images. DF images were obtained by using several reflections (both spotlike and streaked) together around the 210 reflection. Because the reflections were too close to each other in the ED pattern and the objective aperture utilized here was too large to select one or two of them, it was not determined which diffraction spots were really used for the DF imaging. However, 110, 210, 310, 120, 220, and 320 reflections were selected together in every case.

Figure 4 shows an example of the DF images. In this image, dark flecks aligned in lines which are radiating from the center of the single crystal were observed. A slight indication of sectorization was recognized in the radiating manner of the flecks, but a well-defined sector boundary, which is seen, for example, in the polyethylene (PE) single crystal,[13] is not observed. In some DF images, as in Figure 4, irregularly spaced striations which intersect and pass through the flecks are running in the direction parallel to the *b*-axis of the crystal. These striations are clearly seen also in the original negatives, and hence they are not an artifact introduced in the process of photographic duplication. The longest striation measured more than 2.7 μm. It is presumed that the origin of the striations is the stacking faults, and the position of a striation corresponds to that of the fault. Computer simulation for the DF imaging well supported this hypothesis.

Parts a and b of Figure 5, show, respectively, the model structure (*i.e.*, the projected potential distribution of the imaginary crystal) used for the simulation and its Fourier transform. (Note the similarity between the HREM image shown in Figure 3 and the model structure in Figure 5a, especially in the arrangement of the dots along the ⟨120⟩ directions.) In Figure 5a, positions of stacking faults are indicated with arrowheads. If only a streaked reflection, for example 210, is used to

simulate the DF image, the image shows bright striations at the positions of stacking faults. On the other hand, if a spotlike reflection is used, for example 220, striations appear regardless of the location of the stacking faults in the simulated image. When several reflections (both streaked and spotlike) are used together (Figure 5c), the processed image shows bright (or dark) contrast at the positions of stacking faults, as in Figure 5d. Whether the contrast is bright or dark depends on the rotational orientation of the molecules at the fault, that is, if the −AA− type fault appears with bright contrast, then the −BB− type appears with dark contrast. The real DF images in question were taken by using several reflections together. The last case of the simulation (Figure 5c,d), therefore, corresponds to the real DF imaging experiment. The detail of the crystal structure, of course, seems to be smeared and not resolved in the real DF images. Actually the fine structure which appeared in the simulation could not be recognized in the real DF images. However, we can estimate the probability of the presence of the stacking faults from the DF images by counting the number of striations in a certain unit length along the *a*-axis, and the evaluation is now in progress. Preliminary results show that the probability thus estimated from DF images is 17% for the crystal grown at 205 °C and 22% and 28% for the crystals grown at 165 °C.[14]

In each of the DF images (for example, Figure 4), discontinuity of the striations was hardly seen. Hence the faulted plane is long enough along the *b*-axis, as assumed in the analysis of the ED pattern.[12] This result indicates that the stacking fault influences attachment of a new polymer segment as a stem onto the growth face which is not parallel to the *bc*-plane. By combination of this result with the fact that well-defined sectorization was not observed, it is deduced that the polymer chains are folded in an irregular manner even in the single crystals of s-PS. Our additional experiments were consistent with this deduction. (1) When the s-PS crystals were decorated with vapor-deposited PE,[13] the rodlike PE crystals oriented randomly on the fold surface of the s-PS crystals. (2) When the poly(ethylene terephthalate) film on which the s-PS crystals had been deposited was stretched, then small fibrils were observed across the cracks developed in the crystals, but the relative frequency of presence of such fibrils was independent of the orientation of the cracks. (3) When the fold surface of the s-PS crystal lamellae was investigated in the lateral force mode by atomic force microscopy (AFM), no difference was detected between parallel and perpendicular directions to the growth face of the lamellae.

Concluding Remarks

The β-form single crystals of s-PS were grown isothermally from dilute solution at temperatures ranging from 150 to 210 °C. Their ED patterns evidenced that every single crystal inevitably contains the stacking faults. To identify the location of the faults, HREM and DF images of the s-PS single crystals were taken. The shift or kink of (210) lattice fringes, which is along the *b*-direction and corresponds to the position of the stacking fault, was detected in the HREM images. On the other hand, DF images taken using several reflections exhibited irregularly spaced striations which run in the direction parallel to the *b*-axis. It was confirmed from computer simulation based on the structural model of the stacking fault that each striation directly illustrates the position of the stacking fault. Since the striations are continuous over a very long range along the *b*-direction, it is assumed that the stacking fault influences the attachment of a new polymer segment (*viz.* a new stem) onto the growth face which is not parallel to the *bc*-plane, resulting in an irregular fold scheme of the polymer chain, namely in irregular fold-surfaces of the β-form single crystals of s-PS. In our following paper,[14] quantification of the faults in the single crystal will be reported.

Acknowledgment. The authors are grateful to Idemitsu Petrochemical Co., Ltd., for providing the s-PS samples used in this study.

References and Notes

(1) Grassi, A.; Longo, P.; Guerra, G. *Makromol. Chem., Rapid Commun.* **1989**, *10*, 687.

(2) Guerra, G.; Musto, P.; Karasz, F. E.; MacKnight, W. J. *Makromol. Chem.* **1990**, *191*, 2111.

(3) Guerra, G.; Vitagliano, V. M.; De Rosa, C.; Petraccone, V.; Corradini, P. *Macromolecules* **1990**, *23*, 1539.

(4) Gomez, M. A.; Tonelli, A. E. *Macromolecules* **1991**, *24*, 3533.

(5) Wang, Y. K.; Savage, J. D.; Yang, D.; Hsu, S. L. *Macromolecules* **1992**, *25*, 3659.

(6) Capitani, D.; De Rosa, C.; Ferrando, A.; Grassi, A.; Segre, A. L. *Macromolecules* **1992**, *25*, 3874.

(7) Chatani, Y.; Shimane, Y.; Inoue, Y.; Inagaki, T.; Ishioka, T.; Ijitsu, T.; Yukinari, T. *Polymer* **1992**, *33*, 488.

(8) Deberdt, F.; Berghmans, H. *Polymer* **1993**, *34*, 2192.

(9) Kellar, E. J. C.; Galiotis, C.; Andrews, E. H. *Macromolecules* **1996**, *29*, 3515.

(10) Chatani, Y.; Shimane, Y.; Ijitsu, T.; Yukinari, T. *Polymer* **1993**, *34*, 1625.

(11) De Rosa, C.; Rapacciuolo, M.; Guerra, G.; Petraccone, V.; Corradini, P. *Polymer* **1992**, *33*, 1423.

(12) Tsuji, M.; Okihara, T.; Tosaka, M.; Kawaguchi, A.; Katayama, K. *MSA Bull.* **1993**, *23*, 57.

(13) Lotz, B.; Wittmann, J. C. Structure and Properties of Polymers. Chapter 3 in *Materials Science and Technology*; Thomas, E. L., Ed.; VCH: Weinheim, Germany 1993; Vol. 12, pp 79−151.

(14) Hamada, N.; Tosaka, M.; Tsuji, M.; Kohjiya, S.; Katayama, K. Submitted for publication to *Macromolecules*.

MA970024Z